DOI: 10.1002/chem.200600774

O–O Bond Formation in the S_4 State of the Oxygen-Evolving Complex in Photosystem II

Per E. M. Siegbahn*[a]

Abstract: Based on recent X-ray structures of the oxygen-evolving complex in photosystem II, quantum chemical geometry optimizations of several thousand structures have been performed in order to elucidate the mechanism for dioxygen formation. Many of the results of these calculations have been presented previously. The energetically most stable structure of the S_4 state has been used in the present study to investigate essentially all the possible ways the O–O bond can be formed in this structure. A key feature, emphasized previously, of the S_4 state is that an oxygen radical ligand is present rather than an Mn^V state. Previous studies have indicated that this oxygen radical can form an O–O bond by an attack from a water molecule in the second coordination shell. The present systematic investigation has led to a new type of mechanism that is significantly favored over the previous one. A calculated transition-state barrier of 12.5 kcal mol^{-1} was found for this mechanism, whereas the best previous results gave 18–20 kcal mol^{-1}. A requirement on the spin alignment for a low barrier is formulated.

Keywords: density functional calculations · dioxygen · manganese · photosynthesis · reaction mechanisms

Introduction

During the past five years, X-ray crystallography analysis has provided more and more detailed atomistic information of the oxygen-evolving complex (OEC) in photosystem II (PSII). Zouni et al. were the first to obtain crystals that defract at a reasonable, although low, resolution of 3.2–3.8 Å.[1] From their analyses, relative positions of the four manganese centers could be suggested. Similar information was later obtained from an X-ray structure elucidated by Kamiya and Shen.[2] A major breakthrough came a few years later when Ferreira et al. were able to also assign the position of the calcium atom in the OEC as well as the general shape of the complex, even though the resolution was still low at 3.5 Å.[3] A cube formed by three manganese atoms and one calcium atom connected by μ-oxo bonds with the fourth manganese atom outside the cube was suggested from their analysis, which also used previous important results from extended X-ray absorption fine structure (EXAFS) spectroscopy.[4] A reasonable assignment of the ligand structure around the OEC was also made for the first time. Recently, a new X-ray analysis by Loll et al.,[5] based on a slightly higher resolution of 3.0 Å, confirmed the general structure of the OEC. Interesting modifications of the structure were also suggested from their analysis.

Quantum chemical calculations on the mechanism of dioxygen formation in PSII were started long before the first X-ray structures appeared.[6,7] Very general information available from a variety of spectroscopies were used to set up models from which the most fundamental aspects of O–O bond formation could start to be investigated. EXAFS data for Mn–Mn distances in different S states was particularly important in this context.[4] A model with two manganese atoms and a calcium atom connected by μ-oxo bonds in a cube could be set up as a model. There was not enough information to suggest the position of all manganese atoms, and one of them was therefore left out of the model. Furthermore, as it later turned out, the third manganese atom was misplaced. The main result of these studies is that the formation of an oxygen radical ligand appears to be critical for O–O bond formation. O–O bond formation was suggested to occur by an attack of a second-sphere water molecule on the oxygen radical ligand. It should perhaps be clarified

[a] Prof. P. E. M. Siegbahn
Department of Physics, Stockholm University
AlbaNova University Center, Stockholm Center for Physics
Astronomy and Biotechnology, 106 91 Stockholm (Sweden)
Fax: (+46) 8-5537-8601
E-mail: ps@physto.se

Supporting information (containing some of the transition-state values) for this article is available on the WWW under http://www.chemeurj.org/ or from the author.

that for an $(MnO)^{3+}$ moiety there are two possible states: Mn^{V}=O and Mn^{IV}–O(oxyl). The wave functions of these states are quite different and easily distinguished in the calculations. The Mn^{IV}–O(oxyl) state has nearly one unpaired spin on the oxygen atom and about three unpaired electrons on the manganese atom. The Mn^{V}=O state has a rather small spin population on the oxygen atom and only about two unpaired spins on the manganese atom. Which state is lowest in energy depends on the ligand field from case to case. Only the oxyl radical state is reactive enough to form an O–O bond with a low enough barrier.

After the appearance of the X-ray structures mentioned above, much more detailed and therefore more realistic studies of the PSII mechanism could be undertaken. At present, many more than a thousand structures have been optimized at the highest possible level with complete geometry optimizations by using the B3LYP hybrid density functional theory (DFT) method.[8] This method has been shown by benchmark tests to be the most reliable DFT method for computing relative energies.[9] Most results of these optimizations have been reported previously.[10,11,12] The present results are based on the old findings in addition to a few hundred new optimizations.

The emphasis in the more recent of the above-mentioned DFT studies has been on the thermodynamics of the entire reaction cycle.[10,11,12] As the present methodology cannot be used to accurately obtain energetics for charge separations such as protonations and electron transfer, a semiempirical scheme was adopted. In this scheme an experimentally based estimate for the total exergonicity of the entire cycle was used. One more parameter has to be used to enable the thermodynamic cycle to be set up, and this parameter was selected to put the overall energetics in as much agreement with experimental observations as possible. The most important of these observations is the fact that each S state must lie energetically lower than the previous one to drive the process forwards. With these two parameters an energetically reasonable catalytic cycle could be constructed.

In the above-mentioned studies, O–O bond formation was reinvestigated at different stages of the model development. Because no completely systematic study of O–O bond formation has been reported, it was decided that such a study should be undertaken and the results are presented here. By taking the energetically most favorable structure obtained for the S_4 state, essentially all the possible ways of forming the O–O bond have been investigated. Hillier and Messinger have written a recent thorough and interesting survey of different mechanistic alternatives and the reader is referred to this review for further details.[13] The mechanistic alternatives investigated clearly include the water attack on the oxygen radical ligand using different water molecules, and also new pathways and pathways that were earlier considered as very unlikely. This includes, for example, the attack of a nucleophilic water molecule bound to a calcium atom, on an electrophilic Mn^{V}=O ligand, which has been the main mechanism suggested based on experimental information.[14,15] In the examination of different mechanistic alternatives described below, an important energy parameter to keep in mind is the barrier for the rate-determining step in dioxygen formation in PSII. As this is a process that occurs on a timescale of milliseconds, the barrier for O–O bond formation should not be higher than 13–15 kcal mol^{-1} according to transition-state (TS) theory. It is likely, but not clear at present, that O–O bond formation is part of the rate-limiting step.

Computational Methods

In the present study, the starting coordinates of the oxygen-evolving complex were taken from the X-ray structure 1S5L,[3] and then optimized. Modifications of the geometry were then made as described below. Computational models were designed by only selecting ligands that were directly coordinating to the metal cluster. Glutamate and aspartate ligands were modeled as formic acids and the histidines as imidazoles, in line with the modeling of other enzymes.[16] All atoms in the complex were fully optimized, unlike the procedure in previous studies in which some atoms were frozen at their suggested X-ray positions. The reason for this change of strategy is that it was discovered that an unreasonable amount of strain was present in the OEC complex. For other enzyme structures obtained at high resolution, the strain has been found to be very small in general, and the strain obtained for the OEC was therefore considered to be an artifact of the low resolution. Another reason not to fix any atoms suggested from the X-ray structure is that radiation damage may have caused changes of the real structure.[17]

The calculations discussed here were obtained by using the DFT hybrid functional B3LYP[8] with procedures very similar to those used in previous studies.[16,10,11,12] Small basis sets for the geometries, large basis sets for energies, and a surrounding dielectric medium with a dielectric constant equal to 4.0 were used. The main difference is that in the present study a larger basis set cc-pvtz(-f) was used for the final energies rather than the lacv3p** basis set used previously. The metal atoms were still described by using the lacv3p** basis set. Furthermore, the dielectric effects were computed with a lacvp* basis set rather than the lacvp basis set as before. No significant improvement is expected due to these basis set extensions. Even though the use of small basis sets for the geometry optimization has been tested on numerous occasions, still another test was made in the present study. For the best mechanism obtained, the barrier was recomputed with geometries optimized with the lacvp* basis set. The effect was found to be quite marginal as described below. Unlike previous studies in which the metal atoms were ferromagnetically coupled, the present study also systematically considers antiferromagnetic coupling. The accuracy aimed at for the present energies is 3–5 kcal mol^{-1}. This accuracy was, for example, obtained in a recent comparison of experimental and theoretical MnO–H bond strengths for six different complexes.[18] For geometries, the most relevant comparison has been made for a synthetic $Mn^{III,IV,IV,IV}$-cubane structure with oxo bridges.[19] The calculated Mn–Mn distances were on average found to be 0.11 Å longer than the distances given by X-ray diffraction analyses. In particular, the computed Jahn–Teller distortions seem to be overestimated. In the X-ray structure, the longest Mn^{III}–oxo distance is 2.05 Å whereas it is 2.22 Å in the B3LYP optimization. The calculations reported here were all performed by using the program Jaguar.[20]

Results and Discussion

The previous B3LYP studies of the thermodynamic cycle of PSII have involved optimizations of thousands of different structures. The major part of these optimizations has been concerned with finding the best energy structure for each

redox state of the oxygen-evolving cluster. In the so-called Kok cycle there are five S states, numbered from S_0 to S_4. One electron is removed from the OEC between the S states and O_2 is released in the $S_4 \rightarrow S_0$ transition. For each one of these S states, models of the OEC with a total charge of +1, 0, and −1 have been optimized. An important finding in the present context is that the barrier for O–O bond formation is very insensitive to the total charge of the cluster. States of the OEC with absolute total charges higher than 1 can be imagined but appear less likely in the low-dielectric environment of the enzyme interior. Charges of −2 and lower would tend to make electron removal from the cluster very easy, which does not seem reasonable if the full power of the high redox potential of the chlorophyll pigment P680 in the core of PSII should be used. Furthermore, in the modeling studies it has been found that the thermodynamic cycle appears most reasonable if O–O bond formation occurs with a rather low number of protons on the water-derived ligands. A charge state of +2 or more would not be in line with such findings. Each state of the optimized OEC will here be labeled as S_n^m in which n is the S state number and m the charge of the model. Even though O–O bond formation has occasionally been suggested to occur already in the S_3 state, it is generally agreed that it does occur in the S_4 state, only slightly before O_2 is released. In the present context of O–O bond formation, the most interesting structures of the OEC are those of the S_4^{-1} state, and this is the state solely investigated in the present study.

Having decided which formal state should be used for the investigation of O–O bond formation, there is still the question of the general shape, that is, the positioning of the metal atoms, of the complex. The recent X-ray structures agree that one part of the cluster is a cubanelike Mn_3Ca complex in which the metal atoms are connected with μ-oxo bridges. The main debate has been concerned with the positioning of the fourth manganese atom outside the cube; three different suggestions are shown in Figure 1. The first one (**A**) is derived from the original suggestion by Ferreira et al., but the bicarbonate ligand has been replaced by a hydroxide bridge between the outer manganese atom and the calcium atom, see below. In this structure, the fourth manganese atom binds directly to a μ-oxo bridge of the cube. In the second structure (**B**), suggested by Loll et al., the fourth manganese atom does not have any contact with any μ-oxo bridge and instead sticks out directly from one of the manganese centers in the cube and is connected to it by a single μ-oxo bond. The third structure (**C**) is similar to **A** but does not have the fourth manganese atom connected to the calcium atom. Other alternatives for the OEC exist,[21] but these three variants could be said to be representative of the main possibilities. An important comment concerning the X-ray structures is that they are probably all obtained from very reduced samples, maybe with all of the metal atoms in an Mn^{II} oxidation state.[17] A different positioning of the outer manganese atom for a more oxidized cluster would not be surprising because oxidation can affect the protonation states of the connecting ligands.

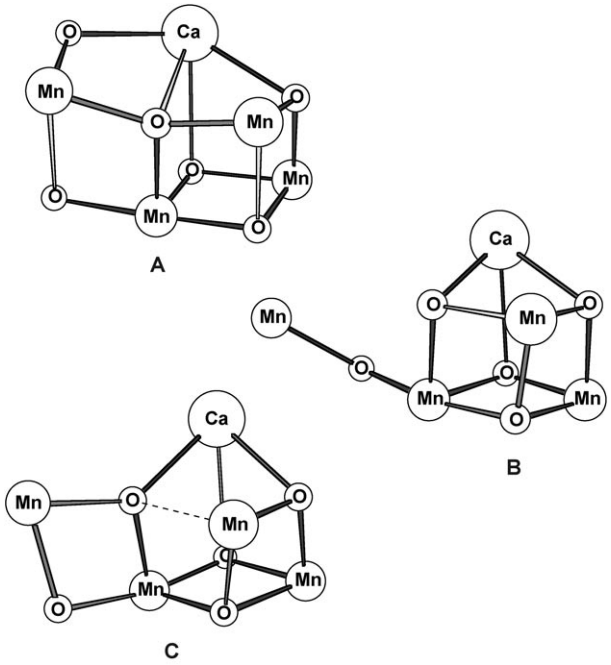

Figure 1. The three different cluster types investigated.

There are more question marks concerning the details of the ligand structure. First, water-derived ligands cannot be seen at the resolution of the crystals of the X-ray crystal diffraction analysis. Second, most of the carboxylate ligands suggested by Ferreira et al. to be terminally bound to a single manganese center in the X-ray structure have in the recent X-ray structure of Loll et al. been assigned as bridging between two metals. Both these assignments have to be regarded as tentative at the present low resolution. Oxidation may also affect the binding modes of the ligands. For example, a carboxylate ligand bidentately binding to a single metal center is very unlikely beyond Mn^{II}. For the present modeling, some assumptions therefore had to be made. The starting point was the cluster suggested by Ferreira et al. However, in a previous paper describing one of the earlier DFT investigations, one conclusion was that the positioning of a bicarbonate ligand between the outer manganese atom and the calcium atom is unlikely,[12] and this ligand has therefore been replaced by an OH^- anion for the present study. In addition, the bicarbonate ligand is not present in the more recent X-ray structure either. Furthermore, water-derived ligands were added to the suggestions made by Ferreira et al. so that each manganese atom was hexacoordinate. The calcium atom was made octacoordinate. The model complex was then fully optimized for each state without constraints. One of the major results of the previous DFT studies is that the mechanism for O–O bond formation is not very sensitive to the ligand structure. At the end of the present study, a dramatic simplification of the ligand structure was made, which demonstrated that the suggested O–O bond-formation mechanism remained the same (see below). Support for a low sensitivity of the mechanism to

the ligand structure also comes from mutation experiments, in which no charge-conserving mutations were found to significantly change the rate of the catalytic cycle.[22,23] The robustness of the OEC cluster in this respect is one of the major surprises in PSII research, and constitutes a fortunate circumstance in the present modeling context. Here, a significant change of the rate is meant as one that changes the free-energy barrier by at least 3 kcal mol^{-1}, which means a rate change of 100. It should be remembered that the accuracy of the hybrid functional B3LYP is not higher than 3–5 kcal mol^{-1} for barriers of chemical reactions. The barriers are nearly always too high for the present type of bond formations calculated by using B3LYP.[24]

Optimal structure: The most stable S_4 complex resulting from the large number of optimizations of different types of OEC clusters is shown in Figure 2. This complex has a total

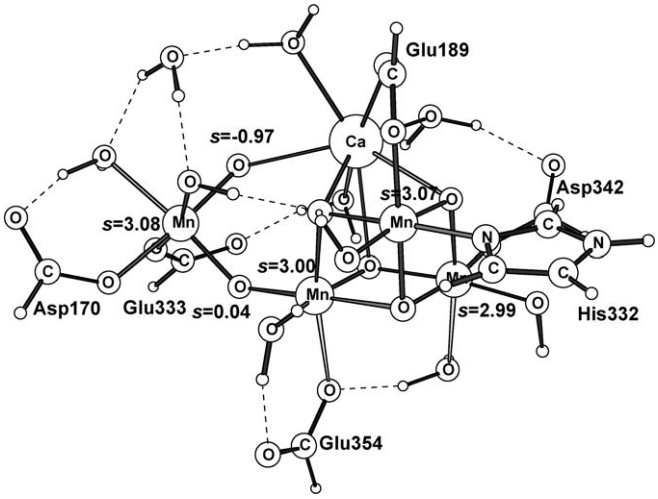

Figure 2. Optimized geometry for the S_4^{-1} state of the OEC.

charge of −1 and the optimization was performed with ferromagnetic coupling between the manganese atoms. The energetic differences between many of the most stable clusters are not large, and the final assignment of this complex as the most stable one is not definitive. One possibility, which was investigated in particular, is whether the outer manganese atom has contact with a μ-oxo bridge. In the lower S states, the clusters both with and without a μ-oxo contact are very similar in energy, within a few kcal mol^{-1}. Therefore, the question of the different assignments of the experimental X-ray structures for the highly reduced clusters cannot be resolved. However, as the cluster is oxidized to the S_4 state, the more open cluster without a μ-oxo contact becomes favored by more than 10 kcal mol^{-1}. Moreover, if the more compact cluster with a μ-oxo contact is optimized in the S_3 state, it rearranges to the more open form with only a low barrier of 2 kcal mol^{-1}. A fully optimized transition state for this rearrangement has been located. The possibility that a complex gets stuck in the more compact structure therefore does not seem likely. For the present purpose, this is the most important aspect of the general shape of the S_4 complex.

By far the most important electronic structure feature of the S_4 state is the presence of an oxygen radical. In many of the previous DFT investigations, this has been suggested to be a critical property for a complex in which the O–O bond formation should occur with a reasonably low barrier. Attempts to obtain an Mn^V solution automatically led to an Mn^{IV} solution with an oxyl radical. To clarify further: if an oxyl radical solution is found, this solution is the lowest in energy. It is then technically impossible to find the higher-lying Mn^V=O solution. The optimal position of the oxyl radical is in between the outer manganese atom and the calcium atom. However, the binding between the oxyl ligand and the calcium atom is rather weak, and a structure without this contact was found to be only 2.8 kcal mol^{-1} higher in energy. With ferromagnetic coupling between the manganese atoms with spins up, the optimal spin orientation of the oxyl radical is with its spin down. The energy difference of the state with the oxyl radical spin up is 1.8 kcal mol^{-1}. With spin correction (spin projection),[25] this difference becomes 2.4 kcal mol^{-1}.

Several states with spin couplings different to those described above have also been determined. If the outer manganese atom (Mn4 in Figure 3) has spin down and the oxyl

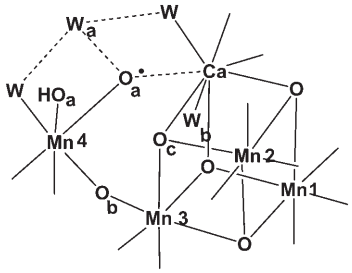

Figure 3. Schematic picture of the OEC showing the labeling of the manganese atoms and the relevant oxygen atoms. For the full structure, see Figure 2.

radical spin up, the energy goes down by 0.2 kcal mol^{-1}. The energy involved in spin coupling of these two atoms with the rest of the cluster is apparently very small. In fact, the energy effect of 0.2 kcal mol^{-1} is close to the convergence threshold used for the geometry optimization. Instead, by just changing Mn2 in the cube to spin down, the spin coupling of the structure shown in Figure 2 causes the energy to increase by 1.0 kcal mol^{-1}. Also, the energy involved in spin coupling within the cube is clearly very small. With Mn2 spin down and the oxyl radical spin up the energy goes up by 2.6 kcal mol^{-1}. Most of this is due to ferromagnetic coupling between the oxyl radical and the outer manganese atom. Similarly, with Mn3 spin down and the oxyl radical spin up the energy goes up by 2.1 kcal mol^{-1} due to the ferromagnetic coupling of the oxyl radical and the outer manganese atom. Other couplings show similar behavior. The

conclusion is that ferromagnetic coupling between the manganese atoms is a good approximation for the S_4 ground state. This conclusion was also reached in all our previous studies based on similar comparisons.

O–O bond-formation barriers: Even if the optimal cluster of the S_4 state still has some uncertainties, it should be sufficiently representative for investigating different mechanistic alternatives for O–O bond formation. In our previous studies of this mechanism, an initial investigation was always performed to sort out those mechanisms that did not appear promising. Only the main alternatives were then followed all the way to a transition-state determination. In contrast, in the present investigation it was decided to follow essentially all possible pathways involving the oxyl radical. Even though there are disagreements as to whether an oxyl radical is actually formed in S_4 prior to O–O bond formation, there is agreement that such a radical should be more reactive than an Mn^V=O species. Therefore, the computed barrier involving an oxyl radical should represent a lower bound for the real barrier, within the present structural model.

To define the reaction mechanisms investigated, a schematic picture of the model used here for the S_4 state of the oxygen-evolving complex is shown in Figure 3. The orientation of this figure is the same as that of the optimized S_4^{-1} state in Figure 2, in which all the details of the ligand structure are shown. In the schematic picture the oxyl radical is labeled O_a. This oxygen atom can easily reach the oxygen atom of another μ-oxo ligand, O_b, which is 2.6 Å away bridging Mn4 and Mn3. One of the bridging oxygen atoms in the Mn_3Ca cube, O_c, which is 3.2 Å away, can also be reached after some minor rearrangement. The oxyl radical can also reach a hydroxyl ligand, HO_a, which is 2.5 Å away on the outer manganese atom, as well as the oxygen atoms of two water molecules, W_a and W_b. Molecule W_b, 2.8 Å away, is a ligand on a calcium atom, whereas W_a, 2.9 Å away, is a second-sphere water molecule held to the cluster by hydrogen bonds. For each oxygen atom that approaches the oxyl radical, two spin states have initially been considered, the HS (high-spin) state in which the oxyl-radical spin is parallel to all the manganese spins, and the LS (low-spin) state in which the oxyl radical has spin down. The manganese atom spins are all held parallel (ferromagnetically coupled) at this stage. The general features of the HS and LS pathways have been described in detail previously.[10,11,12] When the manganese atom spins are ferromagnetically coupled, the HS state is the ground state of the product where the O–O bond is formed. The LS product state has a locally excited medium spin state of one of the manganese atoms. A typical excitation energy is around 15 kcal mol^{-1}. O–O bond formation is approximately thermoneutral, which means that the LS pathway cannot have a barrier lower than this excitation energy. The LS state of the reactant is the ground state but it is only a few kcal mol^{-1} lower in energy than the HS state. For both the LS and HS pathways, a spin transition is normally required, which has been discussed in detail in previous investigations. The spin transition is normally facile and not rate determining.

The resulting barriers for all these possible pathways are given in Table 1. The barriers are counted from the LS ground state (shown in Figure 2). For almost all of them a fully optimized transition state was obtained. However, for two of them (numbers 7 and 9) convergence failed and only a lower bound is given. As both these pathways have very high barriers they were not considered to be of enough interest to pursue a full determination further. The lower bound is obtained by following a one-dimensional pathway for which the O–O distance is decreased in steps. This was also the procedure used to determine an initial guess for the full TS optimization (Figure 4).

Table 1. Barriers for O–O bond formation in the S_4^{-1} state of the OEC. The different mechanisms are described by the oxygen atoms that form the O–O bond (the labels of the oxygen atoms are those given in Figure 3).[a]

Number	Mechanism	Spin state[b]	Spins (s)			O–O	Barrier
			O_a	O_x	Mn[c]	[Å]	[kcal mol^{-1}]
1	O_a–W_a	HS	0.15	0.44	3.41 (4)	1.89	21.9
2		LS	0.00	0.33	2.36 (4)	1.78	22.4
3	O_a–W_b	HS	0.17	0.46	3.43 (4)	1.91	20.0
4		LS	−0.03	−0.36	2.42 (4)	1.77	18.0
5	O_a–W_b[d]	LS	−0.07	−0.22	2.35 (4)	1.74	31.5
6	O_a–OH_a	HS	−0.82	0.97	3.82 (4)	2.43	35.9
7		LS					>40
8	O_a–O_b	HS	0.46	−0.1	3.68 (4)	1.93	22.3
9		LS					>30
10	O_a–O_c	HS	0.65	−0.29	3.56 (2)	1.92	19.3
11		LS	−0.41	−0.03	2.65 (2)	1.66	25.9

[a] Ferromagnetic spin coupling has been used between all manganese atoms. [b] The coupling between the spins on the manganese atoms and the spin on the radical on O_a. [c] The number of the manganese atom that accepts an electron is given in parentheses. [d] The Ca–W_b distance was fixed at 2.46 Å.

The results for the mechanisms in Table 1 will be described in the order of the table. The first one is a reaction between the oxyl radical and a second-sphere water molecule, W_a. This is the type of mechanism that has been favored in all our previous investigations. The computed barriers for the HS and LS coupling are very similar with 21.9 and 22.4 kcal mol^{-1}, respectively, which are also very similar in magnitude to what we found in earlier studies. In this mechanism, W_a first loses a proton to a nearby base, in this case HO_a on the outer manganese atom (Mn4). The electron released when the O–O bond is formed goes to Mn4. It should be added that the initial straightforward optimization of this mechanism, using the hydrogen-bonding network of the reactant, led to higher barriers of 36.9 kcal mol^{-1} for HS

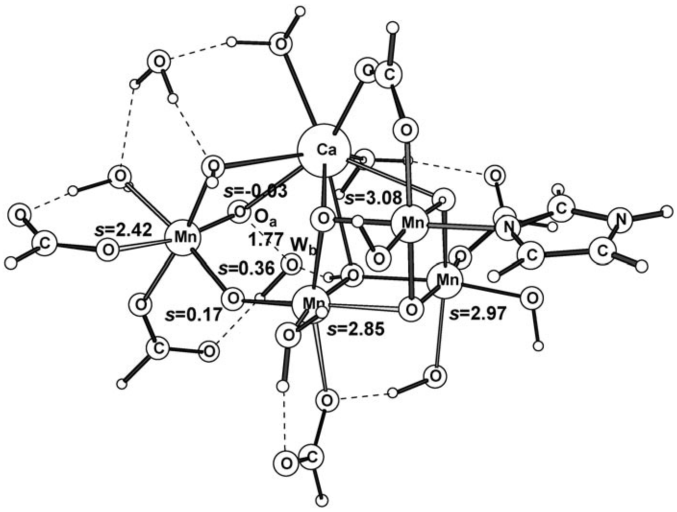

Figure 4. Optimized transition-state geometry for the S_4^{-1} state of the OEC. The oxygen atoms of O_a and W_b form the O–O bond.

and 27.2 kcal mol^{-1} for LS. To lower the barrier, the hydrogen bonding has to change from that of the reactant to an arrangement that can stabilize the free OH group at the stage when the proton has left W_a. This is done by forming a hydrogen bond between the OH group and Glu333. At the HS transition state the O–O bond is 1.89 Å, which is typical for these HS structures, and the spin on the outer manganese atom is 3.41, in between that for Mn^{IV} and Mn^{III}. An important factor in all HS-type mechanisms is the formation of a Jahn–Teller (JT) axis for Mn^{III}. This axis is always formed along the direction of the Mn^{III}–O_2H product and the *trans*-oriented ligand should move outwards. In this case it requires an increase of the Mn4–Asp170 distance from 2.02 Å in the HS reactant to 2.08 Å at the TS. The O–O bond length at the transition state for the LS pathway is shorter than that of the HS state with 1.78 Å and the spin on the outer manganese atom has decreased to 2.36 in the direction of a medium-spin Mn^{III}. For the LS pathway no JT axis is formed.

The next mechanism (number 3) in Table 1 is a reaction between the oxyl radical and a water molecule (W_b) bound to calcium. This mechanism is similar to the one most favored experimentally except that an Mn^{IV}–oxyl group is involved rather than Mn^{V}=O.[14,15] As already mentioned, a reaction with Mn^{V}=O should have a higher barrier than the one computed here. The barrier obtained is somewhat lower than the one involving W_a, with a HS barrier of 20.0 kcal mol^{-1} and a LS barrier of 18.0 kcal mol^{-1}. The base that takes the proton is the bridging μ-oxo group O_c, and the electron released again goes to the outer manganese atom. An important additional point is that at the TS, W_b has left its contact with the calcium atom. In fact, this occurs at a very early stage in the reaction where the distance between the oxyl radical and W_b is still very large and when there is hardly any interaction between these oxygen atoms. At the TS, the electronic structure of W_b is therefore the same as that for W_a in the previous mechanism. This mechanism is therefore in practice not really like the experimental suggestion in which the water molecule should be bound to the calcium atom and its electronic structure modified. The reason that the barrier is lower for the reaction between the oxyl radical and W_b than for the oxyl radical and W_a is that the free OH group formed from W_b after proton release has a more favorable hydrogen-bonding network. For both the HS and LS pathways, the O–O distances and spin distributions at the TS are very similar to the previous mechanism (see Table 1).

To mimic the experimentally suggested mechanism better, the Ca–W_b distance was fixed and not allowed to be varied during the reaction (mechanism 5 in Table 1). In this way, one might hope to change the character of this water molecule, which might be an advantage in O–O bond formation. However, for purely technical reasons one cannot expect that a barrier should be lower when one distance is not allowed to be varied. In fact, the barrier (LS) becomes substantially higher with 31.5 kcal mol^{-1}. For an Mn^{V}=O state it should be even higher. The conclusion is that the change of character of the water molecule, induced by the binding to calcium, is not important for O–O bond formation. The present result is in agreement with our previous studies for other models, where this type of mechanism was eliminated at an early stage and was therefore not completely optimized until now. The conclusion in our previous studies has instead been that the water molecule that makes the attack on the oxyl radical should be as free as possible, because otherwise the bond to which it is attached first needs to be broken, which requires some energy. In the O_a–W_b mechanism without constraints the barrier is only 18.0 kcal mol^{-1}, which is due to the simplicity with which the bond between the calcium atom and W_b is broken. Moving this water molecule from the first to the second coordination sphere of the calcium atom only costs 0.8 kcal mol^{-1}, due to a compensating rearrangement of the other ligands on the calcium atom.

In the next mechanism in Table 1 (number 6), the O–O bond is formed between the oxyl radical and HO_a on the outer manganese atom. The barrier for both HS and LS is very high with 35.9 and over 40 kcal mol^{-1}, respectively. The reason for this is that the bond between OH_a and Mn4 has to be broken during the reaction leading to the O_2H ligand bridging between Ca and Mn4. The product O_2H binds through only one of its oxygen atoms, that is, the one emanating from the oxyl radical. At the HS transition state the Mn4–OH_a bond has already increased from 1.84 to 2.44 Å. The O–O bond at the TS is also very long with 2.43 Å, which indicates a late TS and a difficult O–O bond formation. The electron released goes to the outer manganese atom (Mn4), which obtains a spin of 3.82 at the TS, a value close to that of Mn^{III}.

The remaining mechanisms in Table 1 are quite different from those described above. In these cases the O–O bond is formed between the oxyl radical and a bridging oxo ligand. In the first mechanisms (numbers 8 and 9) the oxo (O_b) bridges between the outer manganese atom and Mn3 in the Mn_3Ca cube. In the other mechanisms (numbers 10 and 11)

the oxo atom (O_c) is one of the bridging oxo ligands in the cube. From the conclusion drawn above, in which the free character of the second-sphere water molecule reacting with the oxyl radical was found to be very favorable, it could be expected that these mechanisms should have rather high barriers, because the oxo ligands are strongly bound to the cluster. On the other hand, no proton needs to be released and no strong base is therefore required. The computed HS barrier of the O_a–O_b mechanism is 22.3 kcal mol^{-1}, which is surprisingly competitive with the best mechanism described so far, although not quite as low. The O–O bond length of 1.93 Å at the TS and the spin distributions are rather similar to the previous ones with one notable exception: the oxygen atom that reacts with the oxyl radical has a negative spin rather than the substantially positive spin for the previous mechanisms. The electron released in the HS pathway again goes to the outer manganese atom, which obtains a spin of 3.68 at the TS. The advantage of this mechanism in not having to release any proton is partly compensated by the problem of having two bonds to the same manganese atom (Mn4). The oxygen atom bridging between Mn3 and Mn4 is forced to increase its distance to Mn4. For the reactant this distance is 1.80 Å, for the TS it is 1.96 Å, and for the product 2.36 Å. For the LS case the barrier becomes very high with more than 30 kcal mol^{-1}. In fact there is not even a local minimum for short O–O distances. In this case the electron is released to Mn3 and not to the outer manganese atom. Because Mn4 keeps its Mn^{IV} oxidation state it wants to keep both bonds to the oxygen atoms, which becomes unfavorable as the O–O bond gets shorter. Furthermore, Mn3 does not want to be reduced to Mn^{III} with its four oxo ligands and one glutamate ligand.

When the O–O bond is formed between the oxyl radical and a bridging oxo ligand in the Mn_3Ca cube (mechanisms 10 and 11), the flexibility of the cluster is a big advantage. While the Mn–O_c bonds in the cluster get weaker as the O–O bond forms, many other bonds can strengthen to compensate for the binding loss. In fact, this makes this mechanism highly competitive with the previous ones. The low HS barrier of 19.3 kcal mol^{-1} is only 1.3 kcal mol^{-1} higher than the best previous one, which was one of the major surprises in the present study. A strongly contributing factor is the favorable JT axis formed in the reaction. The ligand on Mn2 oriented *trans* to the O–O bond formed is His332, which can easily increase its distance. For the reactant this distance is 2.02 Å and at the TS it is 2.13 Å. Also the Mn2–O distance can increase easily by compensating bond formations, as mentioned earlier. The importance of this favorable JT axis will be returned to in the next section, where it becomes even more obvious. The O–O bond length at the TS is 1.92 Å, again typical for the HS case, and the electron is released to Mn2 in the cube, which obtains a spin of 3.56 at the TS. The spin distribution is similar to that of the O_a–O_b mechanism with a negative oxo ligand at the TS with a spin population of −0.29. The LS barrier is much higher with 25.9 kcal mol^{-1}, due to the unfavorable formation of a medium-spin manganese atom in the cube. At the TS, Mn2 obtains a spin of 2.65, at an O–O distance of 1.66 Å.

Antiferromagnetic effects: As described above, the energies involved in spin coupling between the different manganese atoms are very small and only marginally affect the stability of the S_4^{-1} ground state. Therefore, it was initially expected that changing spins on individual manganese atoms should not have any significant effect on the barriers either. This expectation was borne out in the first mechanisms investigated. The results are collected in Table 2, in which the barriers are again counted from the LS ground state with ferromagnetic coupling as shown in Figure 2. The mechanisms in Table 2 should be compared with those in Table 1 in which the absolute value of the spin on the electron-accepting manganese atom goes in the same direction. For example, the first mechanism in Table 2 corresponds to the fourth one (LS) in Table 1 because the absolute value of the spin on Mn4 goes down from 3 to 2.3 (or 2.4). This means that the d electrons on Mn4 become medium-spin coupled, and this is therefore a locally excited state. Whether the electron-accepting manganese atom goes to its high-spin ground state or to its medium-spin excited state in the product is entirely dictated by the choice of spins in the reactant, as described in Table 2 under the heading "Spin-state".

Table 2. Barriers for O–O bond formation in the S_4^{-1} state of the OEC, in which antiferromagnetic spin coupling has been introduced relative to Table 1.[a]

Number	Mechanism	Spin state[b]	Spins (s)			O–O	Barrier
			O_a	O_x	Mn	[Å]	[kcal mol^{-1}]
1	O_a–W_b	Mn4β, O_aα	0.03	0.33	−2.32 (4)	1.78	19.1
2	O_a–O_b	Mn4β, O_aα					>30
3	O_a–O_b	Mn3β, O_aβ	−0.78	0.75	3.90 (4)	2.12	24.1
4	O_a–O_b	Mn3β, O_aβ	−0.48	−0.09	−3.53 (3)	1.79	29.1
5	O_a–O_c	Mn2β, O_aα	0.43	−0.09	−2.42 (2)	1.77	32.4
6	O_a–O_c	Mn3β, O_aβ	−0.48	0.13	−3.39 (3)	1.75	25.1
7	O_a–O_c	Mn2β, O_aβ	−0.61	0.11	−3.52 (2)	1.85	12.5
8	O_a–O_c	Mn4β, O_aα	0.64	−0.23	3.53 (2)	1.85	13.4

[a] Ferromagnetic spin coupling has been used between all manganese atoms except the one specified in the column "Spin state". [b] α denotes spin up and β spin down.

In the first mechanism in Table 2 the spins on the outer manganese atom (Mn4) and O_a are both reversed compared with the best mechanism (number 4) in Table 1, and the bond formation occurs between O_a and the oxygen atom of W_b. The barrier obtained is 19.1 kcal mol^{-1}, compared with 18.0 kcal mol^{-1} for mechanism 4 (Table 1) with ferromagnetic coupling. The spin on Mn4 becomes −2.32 compared with +2.42 with ferromagnetic coupling, and the O–O distance becomes almost the same as before, 1.78 and 1.77 Å, respec-

tively. The best mechanism with ferromagnetic coupling is thus not improved by allowing the manganese spins to change direction. Also, for bond formation between O_a and O_b the results are quite similar to those in Table 1. When the spin on both Mn4 and O_a are reversed (mechanism 2) the barrier remains over 30 kcal mol^{-1} (compare with mechanism 9 in Table 1). When the spin on Mn3 is reversed instead (mechanism 3), the barrier becomes 24.1 kcal mol^{-1} compared with 22.3 kcal mol^{-1} for the corresponding mechanism 8 in Table 1. The electron prefers to go to Mn4 as before. When the electron is forced to go to Mn3 as in mechanism 4, the barrier increases to 29.1 kcal mol^{-1}. The results discussed so far can be summarized as rather small effects that do not change the favored mechanism from being the one in which the bond is formed between O_a and W_b. The barrier is 18–20 kcal mol^{-1} as in our previous investigations.

The first studies of the mechanism in which the bond is formed between O_a and O_c gave similar results to those described above. When the spin on Mn2 is reversed (mechanism 5, Table 2), the barrier becomes 32.4 kcal mol^{-1} compared with 25.9 kcal mol^{-1} for mechanism 11 in Table 1. When the spin on Mn3 is changed instead (mechanism 6), the barrier becomes 25.1 kcal mol^{-1} (no corresponding value in Table 1). Some of the details of these mechanisms will be returned to below.

For mechanism 7 (Table 2), there is a dramatic effect. A barrier of only 12.5 kcal mol^{-1} was found, which is much lower than that found for any mechanism tried so far, in the present or in our earlier studies. For example, this is much lower than that for the corresponding mechanism 10 in Table 1, for which the barrier is 19.3 kcal mol^{-1}. The fully optimized transition state is shown in Figure 5. The geometric structure of this TS is not much different from the one with ferromagnetic coupling. The absolute values of the spins are also quite similar. Like mechanism 7, mechanism 8 also has a low barrier of only 13.4 kcal mol^{-1}. It is clear that these latter mechanisms have something in common that is different from the other mechanisms tried. Because the result obtained for these mechanisms must be considered very important, the barrier for mechanism 7 was recomputed by using geometries optimized with a larger basis set. Optimizing the geometry with the lacvp* basis set led to a decrease of the barrier by 0.5 kcal mol^{-1}, which is a very small effect compared with the uncertainty obtained from using the B3LYP functional. This result was expected based on previous experience.[26]

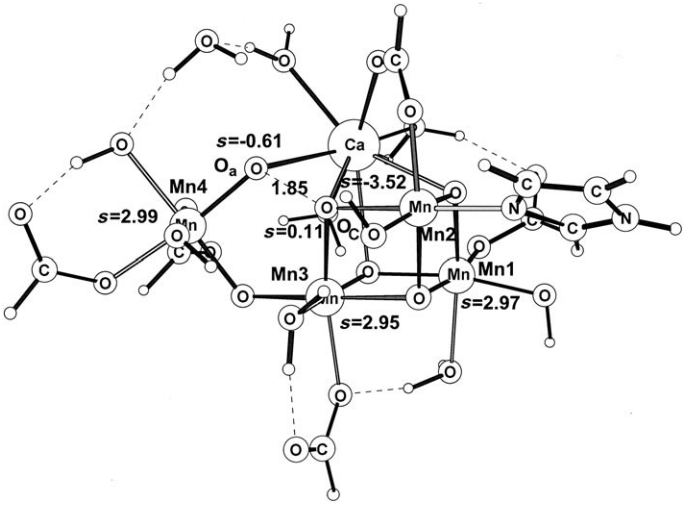

Figure 5. Optimized transition-state geometry for the S_4^{-1} state of the OEC with antiferromagnetic spin coupling. The oxygen atoms O_a and O_c form the O–O bond.

The key difference between the two last mechanisms in Table 2 and all the other mechanisms investigated turns out to be the spin alignment, as described schematically in Figure 6. There is an alternation of the signs of the spins on going from the outer manganese atom Mn4, to O_a, to O_c, and then to Mn2. This means that as the bond is formed this is done with a spin down (β) on O_a and a spin up (α) on O_c. Opposite spins on these oxygen atoms is required because these two electrons should be singlet-paired in the O–O bond. At the same time, O_c should lose spin-down electrons to get an overall spin up, and this is done to Mn2, which has the right overall spin down to incorporate the extra electron released in the O–O bond formation. Mn2 will afterwards have a high-spin coupling of the d electrons, which is the local ground state. This type of electron transfer of electrons with the right spin is present in most mechanisms described above, even those with much higher barriers. The important difference comes in with the alignment with spin up on Mn4 and spin down on O_a. This has been shown to be favored by a few kcal mol^{-1} for the reactant compared with the situation in which these spins are parallel, see above, but is clearly much more important at the transition state, which must be considered a major surprise. The spin alignment in the last two mechanisms are identical on these four atoms. The only difference is that for mechanism 7 the spin on Mn2 is antiparallel to the inactive manganese atoms Mn3 and Mn1 in the cube. Mechanism 8 has these spins parallel, which is slightly disfavored.

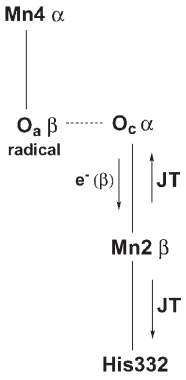

Figure 6. Requirements for a low O–O bond-formation barrier. α and β denote spin directions.

Another important factor for a low barrier is clearly that the electron-accepting manganese atom can easily become Mn^{III}. A key feature of Mn^{III} is its Jahn–Teller axis. The JT axis will always be formed along the bond between manganese and the newly formed O_2, because the Mn–O_2 bond will be unusually weak. Oriented *trans* to this bond for Mn2 in the optimal mechanism is His332, which is a favorable ligand as it is not charged. The Mn2–His332 distance can therefore easily increase during the formation of the JT axis.

An interesting question arises in this context because in the most recent X-ray structure bidentately bridging Asp342 is the *trans* ligand and not His332.[5] It turns out that this is even more favorable for a low barrier, as will be described in detail in a forthcoming study. A bidentately bridging ligand has the advantage that when one of the metal–ligand bonds is weakened by the JT effect, the other one can compensate by becoming stronger.

Having realized the requirement for a low barrier, it is interesting to investigate whether there are any other mechanisms that fulfill the same spin requirement. The most obvious one is mechanism 6, for which the spins on Mn4, O_a, O_b, and Mn3 are alternating (see Table 2). Still the barrier is quite high with 25.1 kcal mol^{-1}. The reason for this is that Mn3 does not want to decrease its positive charge to become Mn^{III} surrounded by its four negative oxo ligands and the negative Glu354. The anionic Glu354 will lie along the JT axis formed, which is also unfavorable compared with having the neutral His332 along the JT axis. Similarly, mechanisms 3 and 4 involving O_a–O_b bond formation, have in principle, a possibility for the right spin alignment but the barriers for these mechanism are still high with 24.1 and 29.1 kcal mol^{-1}, respectively. Mechanism 4 has a high barrier because Mn3 does not want to become Mn^{III}, as mentioned above. For mechanism 3, the outer manganese atom Mn4 takes the electron to become Mn^{III}, which is slightly better. However, in this process the strong Mn4–O_b bond has to be cleaved. At the TS this bond has elongated from 1.79 to 2.29 Å; this leads to a late TS with an O–O bond of 2.12 Å. Considering the possibilities available for the OEC cluster as shown in Figure 2, it is concluded that no additional favorable mechanisms can be expected.

Spin requirements for formation of the O–O bond in manganese complexes have also been discussed by McGrady and Stranger.[27] Their discussion concerns the problem that O–O bond formation may end up in a locally excited manganese state. This problem has been mentioned above, and is avoided in most mechanisms both for the ferromagnetically and antiferromagnetically coupled cases. This important problem has also been extensively discussed in our earlier papers with special emphasis on O–O bond formation involving an oxyl radical.[10,11,12]

Ligand sensitivity: As the exact ligand positioning in the oxygen-evolving complex is still not quite known from the low-resolution X-ray experiments, it is interesting to try to investigate the sensitivity of the barrier to the ligand choice. It is known that the results are in general quite insensitive to the choice of models of the amino acids.[26] For example, choosing formate or acetate as a model for glutamate, in general, gives very similar energetic results (within 1 kcal mol^{-1}) for reactions of the present type. In fact, drastic modeling of histidine with ammonia instead of imidazole gives a surprisingly accurate account of the electronic effects. For the present case, a model was studied in which every neutral ligand was chosen as water and every negatively charged one as OH^-. It should be emphasized that these are all charge-conserving modifications. For the specific carboxylate (Glu189) that bridges between the calcium and manganese atoms, a water molecule was put on the calcium atom and OH^- on the manganese atom. The geometries of this very simplified model were fully reoptimized and new dielectric and zero-point effects were computed. The barrier for the best mechanism described above was computed to be 10.5 kcal mol^{-1} compared with 12.5 kcal mol^{-1} for the more realistic model, a difference of only 2.0 kcal mol^{-1}. The conclusion is that the mechanism and the barrier height are quite insensitive to the precise ligand choice.

Functional stability: The most sensitive parameter of the B3LYP functional is the amount of exact exchange included. This parameter is 20% in B3LYP and 0% in pure density functionals like BLYP. To get an idea of the sensitivity of the present results, the most important barriers were recomputed with 15% exact exchange, which has been suggested to be a better choice for transition metals than the standard 20%.[28] The general experience is that this will lower most barriers for chemical reactions including the one for O–O bond cleavage (and formation).[24] Furthermore, when the effect is significant the result with 15% is probably better. The geometries were kept the same as those optimized with standard B3LYP, as well as the dielectric and zero-point vibrational effects. For the most important case with the lowest barrier of 12.5 kcal mol^{-1} (number 7 in Table 2), 15% exact exchange gave a moderate decrease of only 1.0 kcal mol^{-1} to 11.5 kcal mol^{-1}. This is considered to be a very stable result with respect to the functional choice. For the lowest barrier with ferromagnetic coupling between all manganese atoms (number 4 in Table 1), the effect was somewhat larger with a lowering of 3.0 kcal mol^{-1}, from 18.0 to 15.0 kcal mol^{-1}. The conclusion is that the mechanism involving antiferromagnetic coupling described above is very stable to the functional used and remains substantially better than the other mechanisms tried.

Another technical comment could also be made at this stage. In the mechanism described above, the eigenvalue of S^2 is clearly not well defined along the reaction pathway. The single determinantal nature of the B3LYP wave function will lead to a mixture of several states with different spin eigenvalues. Because all other determinants will have higher barriers, mixing the present determinant with these would only lower the barrier further. The general experience is that this might lower the barrier by 3–5 kcal mol^{-1}.[24] A major advantage of the present single determinant description is that the origin of the low barrier, as described above, is much easier to understand than it is for a multiconfigurational wave function, for which a large number of configurations will probably have substantial weights of different magnitudes. However, such a multireference wave function with sufficient accuracy would, at the present stage anyway, be impossible to obtain.

Conclusions

A large number of geometry optimizations of different possible structures of the oxygen-evolving complex in photosystem II have been performed during the past years, based on available X-ray structures. In the present study, the lowest-energy S_4 structure obtained (see Figure 2) has been used to investigate all possible O–O bond-formation mechanisms for this particular cluster. This led to the surprising result that one pathway stands out, one not previously studied or suggested. In this mechanism, the oxyl radical bound to the dangling manganese atom forms the O–O bond to a bridging oxo ligand in the Mn_3Ca cube. A key feature in the mechanism is that the spins involved alternate for all atoms involved, from the outer manganese atom, to the oxyl radical, to the oxo ligand, and finally to the manganese atom in the cube (see Figure 6). This alignment fulfills the usual requirement that the spins on the oxygen atoms have different directions as the bond is formed. A surprising point is that the antiparallel spin alignment between the outer manganese atom and the oxyl radical is much more important for the transition state than for the reactant even though the spin population is higher on the oxyl of the reactant. Another important feature of the best mechanism is that a good Jahn–Teller axis is formed on Mn2 as it has a neutral histidine ligand (His332) oriented *trans* to the O–O bond being formed. Having a bidentately bridging carboxylate molecule (Asp342) as the *trans* ligand, which is the case in the most recent X-ray structure,[5] turns out to be even better in this respect.

One reason the present mechanism was not found in previous investigations is that the O–O bond formation occurs precisely where a bicarbonate ligand was placed in the X-ray structure.[3] While the positioning of a bicarbonate ligand may still be true for the reduced cluster in the X-ray crystal, its position in S_4 would prevent the presently suggested mechanism. The positioning of a bicarbonate ligand between the calcium atom and the dangling manganese atom was questioned in one of our more recent investigations, because this led to a redox potential that was too high for the S_3 state of the cluster,[11] and it was therefore removed in the present study. A second problem to be overcome to reach the present mechanism was that the originally suggested X-ray structure had a direct contact between the outer manganese atom (Mn4) and an oxo ligand in the cube. Again, while this is still a possibility for a reduced cluster, this would also prevent the present mechanism.

Because essentially only one low-barrier mechanism appears to be present for the OEC cluster, it is possible to rationalize some of the structural features of this cluster. First, a manganese atom is required to hold the oxyl radical produced in the S_3 to S_4 transition. As the oxyl radical should form the bond with an oxo ligand in the cube, this sterically forces the oxyl-binding manganese atom to be outside the cube and not bind directly to any oxo ligand in the cube. Second, the other oxygen partner in the O–O bond formation should be involved in a network of bonds that can allow compensating bond formations to occur as the O–O bond is formed, as this process will weaken the bonds between these oxygen atoms and the metal atoms; an oxo ligand in the Mn_3Ca cube is ideal for this purpose. Third, a favorable JT axis needs to be formed for the manganese atom in the cube that accepts the electron released in the O–O bond formation; this is available by having a neutral ligand, or a bidentately bridging carboxylate ligand, on the electron-accepting manganese atom oriented *trans* to the O–O bond formed.

An interesting result is that the computed barrier of 12.5 kcal mol^{-1} is lower than that estimated from experiments.[29] This is initially puzzling because it is a general experience that the present hybrid DFT method B3LYP tends to overestimate this type of barrier by 3–5 kcal mol^{-1}.[24] At the present stage a best estimate of the barrier would thus be 7–9 kcal mol^{-1}. The easiest way to rationalize this apparent conflict with experiments is to conclude that the starting reactant of the present study is not the resting state for O–O bond formation. Indeed, it has recently been shown that the intermediate that occurs before O–O bond formation is one in which an electron has not yet left the OEC.[30] This state can be described as S_3^* Tyr_Z(rad). If the electron transfer to Tyr_Z is uphill by 3–5 kcal mol^{-1}, a reasonable rate for O–O bond formation in the milliseconds range is achieved with an additional O–O bond cleavage barrier of 7–9 kcal mol^{-1}.

The mechanism for O–O bond formation described above can be compared to those previously suggested. The mechanism mostly favored experimentally is one in which a water molecule bound to the calcium atom attacks an Mn^V=O ligand.[14,15] This mechanism is one of those investigated here. On the basis of the present results with a very high barrier of over 30 kcal mol^{-1}, this appears to be an unlikely mechanism. A mechanism much more similar to the present one has been suggested by Messinger, where an OH ligand on the dangling manganese atom attacks a bridging oxo ligand in the Mn_3Ca cube.[31] The argument for one partner in the O–O bond formation being a bridging oxo ligand in Mn_3Ca is that water-exchange experiments with the natural and a strontium-substituted OEC have indicated that the slowly exchanging oxygen atom forming O_2 has a bond to the calcium atom.[32] This experimental finding is clearly also in line with the presently suggested mechanism. The difference between the previously reported mechanism and the mechanism presented here concerns the second oxygen atom making the O–O bond: in the present mechanism this is an oxyl radical bound to Mn^{IV}, rather than a nonradical hydroxide ligand bound to Mn^{III}. The presence of a low-lying state with an oxygen-containing radical for a low O–O bond-formation barrier is the strongest requirement found from the present and our earlier computational studies.

[1] A. Zouni, H.-T. Witt, J. Kern, P. Fromme, N. Krauss, W. Saenger, P. Orth, *Nature* **2001**, *409*, 739–743.

[2] N. Kamiya, J.-R. Shen, *Proc. Natl. Acad. Sci. USA* **2003**, *100*, 98–103.
[3] K. N. Ferreira, T. M. Iverson, K. Maghlaoui, J. Barber, S. Iwata, *Science* **2004**, *303*, 1831–1838.
[4] V. K. Yachandra, K. Sauer, M. P. Klein, *Chem. Rev.* **1996**, *96*, 2927–2950.
[5] B. Loll, J. Kern, W. Saenger, A. Zouni, J. Biesiadka, *Nature* **2005**, *438*, 1040–1044.
[6] P. E. M. Siegbahn, R. H. Crabtree, *J. Am. Chem. Soc.* **1999**, *121*, 117–127.
[7] P. E. M. Siegbahn, *Inorg. Chem.* **2000**, *39*, 2923–2935.
[8] A. D. Becke, *J. Chem. Phys.* **1993**, *98*, 5648–5652.
[9] C. W. Bauschlicher, Jr, A. Ricca, H. Partridge, S. R. Langhoff in *Recent Advances in Density Functional Methods, Part II* (Ed.: D. P. Chong), World Scientific Publishing Company, Singapore, **1997**, p. 165.
[10] M. Lundberg, P. E. M. Siegbahn, *Phys. Chem. Chem. Phys.* **2004**, *6*, 4772–4780.
[11] M. Lundberg, P. E. M. Siegbahn, *Photochem. Photobiol. Sci.* **2005**, *4*, 1035–1043.
[12] P. E. M. Siegbahn, M. Lundberg, *J. Inorg. Biochem.* **2006**, *100*, 1035–1040.
[13] W. Hillier, J. Messinger in *Photosystem II, The Light-Driven Water:-Plastoquinone Oxidoreductase, Advances in Photosynthesis and Respiration, Vol. 22* (Eds.: T. J. Wydrzynski, K. Satoh), Springer, The Netherlands, **2005**, pp. 567–608.
[14] J. P. McEvoy, J. A. Gascon, V. S. Batista, G. W. Brudvig, *Photochem. Photobiol. Sci.* **2005**, *4*, 940–949.
[15] S. Iwata, J. Barber, *Curr. Opin. Struct. Biol.* **2004**, *14*, 447–453.
[16] P. E. M. Siegbahn, *Q. Rev. Biophys.* **2003**, *36*, 91–145.
[17] J. Yano, J. Kern, K.-D. Irrgang, M. J. Latimer, U. Bergmann, P. Glatzel, Y. Pushkar, J. Biesiadka, B. Loll, K. Sauer, J. Messinger, A. Zouni, V. K. Yachandra, *Proc. Natl. Acad. Sci. USA* **2005**, *102*, 12047–12052.
[18] M. Lundberg, P. E. M. Siegbahn, *J. Comput. Chem.* **2005**, *26*, 661–667.
[19] W. F. Ruettinger, D. M. Ho, G. C. Dismukes, *Inorg. Chem.* **1999**, *38*, 1036–1037.
[20] Jaguar 5.5, L. L. C. Schrödinger, Portland, OR, (**1991**–**2003**).
[21] J. Yano, Y. Pushkar, P. Glatzel, A. Lewis, K. Sauer, J. Messinger, U. Bergmann, V. Yachandra, *J. Am. Chem. Soc.* **2005**, *127*, 14974–14975.
[22] P. J. Nixon, M. Sarcina, B. A. Diner in *Photosystem II, The Light-Driven Water:Plastoquinone Oxidoreductase, Advances in Photosynthesis and Respiration, Vol. 22* (Eds.: T. J. Wydrzynski, K. Satoh), Springer, The Netherlands, **2005**, pp. 71–94.
[23] R. Debus in *Photosystem II, The Light-Driven Water:Plastoquinone Oxidoreductase, Vol. 22, Advances in Photosynthesis and Respiration* (Eds.: T. J. Wydrzynski, K. Satoh), Springer, The Netherlands, **2005**, pp. 261–284.
[24] P. E. M. Siegbahn, *J. Bioinorg. Chem.* **2006**, *11*, 695–701, in press.
[25] L. Noodleman, D. A. Case, *Adv. Inorg. Chem.* **1992**, *38*, 423–470.
[26] P. E. M. Siegbahn, *J. Comput. Chem.* **2001**, *22*, 1634–1645.
[27] J. E. McGrady, R. Stranger, *Inorg. Chem.* **1999**, *38*, 550–558.
[28] M. Reiher, O. Salomon, B. A. Hess, *Theor. Chem. Acc.* **2001**, *107*, 48–55.
[29] J. Clausen, W. Junge, *Nature* **2004**, *430*, 480–483.
[30] M. Haumann, P. Liebisch, C. Müller, M. Barra, M. Gabolle, H. Dau, *Science* **2005**, *310*, 1019–1021.
[31] J. Messinger, *Phys. Chem. Chem. Phys.* **2004**, *6*, 4764–4771.
[32] G. Hendry, T. Wydrzynski, *Biochemistry* **2003**, *42*, 6209–6217.

Received: June 2, 2006
Published online: October 9, 2006

